Sediment Trap Records of Glacimarine Sedimentation at Müller Ice Shelf, Lallemand Fjord, Antarctic Peninsula

Authors: Gilbert, Robert, Chong, Åsa, Dunbar, Robert B., and Domack, Eugene W.

Sediment Trap Records of Glacimarine Sedimentation at Müller Ice Shelf, Lallemand Fjord, Antarctic Peninsula

Robert Gilbert,*
Åsa Chong,*
Robert B. Dunbar,†
and Eugene W. Domack‡

*Department of Geography, Queen's University, Kingston, Ontario K7L 3N6, Canada.
gilbert@lake.geog.queensu.ca
†Department of Geological and Environmental Sciences, Stanford University, Stanford, California 94305-2115, U.S.A.
dunbar@stanford.edu
‡Geology Department, Hamilton College, Clinton, New York 13323, U.S.A.
edomack@hamilton.edu

Abstract

Three arrays, each containing four funnel-shaped sediment traps, were deployed near the front of the Müller Ice Shelf, Lallemand Fjord, western Antarctic Peninsula, in late austral summer 1998. Although the upper traps in each array were damaged or lost, eight others were recovered intact about 13 mo later. The mean flux of sediment was 1.4 to 2.9 mm a^{-1} (1.67 to 3.5 kg m^{-2} a^{-1}) and showed little trend with respect to distance from the ice shelf or depth of water. Mean organic carbon and biogenic silica concentrations are 0.6 to 1.1% and 3.4 to 5.0%, respectively. Up to 50 microlaminae visible in x-radiographs probably indicate storm surges or the effect of spring tidal cycles. The sand content in most traps is 2 to 5 times lower in winter, reflecting reduced melt from icebergs and their limited mobility as they are held by sea ice. However, a secondary winter peak in very coarse sand is probably associated with eolian input during winter storms. Nitrogen is greater by 2 to 3 times in summer sediment, and organic carbon is up to 4 times greater. Biogenic silica shows less summer to winter difference, although the spring diatom bloom is represented by somewhat greater values in most traps. Summer values of isotopic organic carbon δ^{13}C and total nitrogen δ^{15}N are lower than winter values in response to heterotrophic removal of the lighter isotopes.

Introduction

Antarctic ice shelves have generated significant scholarly interest related to glacimarine sedimentary environments (Domack and Ishman, 1993) and because many are undergoing rapid, unprecedented retreat associated with changing climate (Skvarca et al., 1999; Domack et al., 2001; Scambos et al., 2001). Müller Ice Shelf at 67°13′S is the most northerly of the ice shelves on the west side of the Antarctic Peninsula. It is preserved because of its sheltered position near the head of Lallemand Fjord (Fig. 1) but is retreating. Because of its small size compared to the other shelves of Antarctica, it may vanish in a few decades. The fjord has been the subject of research for some time, with studies documenting its oceanography, sedimentology, and paleoenvironmental change (Domack et al., 1995; Shevenell et al., 1996). In this paper, we present results from sediment traps deployed for 13 mo from austral summers 1998 to 1999. Our objective is to provide a high-resolution, intra-annual record of variability in sedimentation, not obtainable from cores in this region where the rates of accumulation are too low to allow this resolution. These are the first such results from Antarctic fjords and allow better understanding of the seismic reflection and core data representing longer periods within these settings.

Methods

The study was conducted during U.S. Antarctic Program cruises in 1998 and 1999 aboard research vessels *L. M. Gould* and *N. B. Palmer,* respectively. During the first cruise three arrays of sediment traps were deployed on 3 March 1998 (Fig. 2). Each consisted of four cone-shaped fiberglass traps with baffled openings of either 0.156 (Array A) or 0.138 m^2 (Arrays B and C) and attached to a single tube 44 mm in diameter and 0.3 m

long. This created a concentration factor (the ratio of the area of the mouth of the funnel to the cross-sectional area of the collecting tube) of 100 or 89 times. The traps were moored at the locations shown in Figure 1 and at depths shown in Figure 2, each array with a 200-kg concrete anchor at the bottom and four 0.5-m-diameter floats just above the top trap. To avoid damage by sea ice and shallow-draft icebergs, the uppermost floats were located well below the sea surface. However, a weighted tag line was deployed from the floats about 500 m outward from each array to facilitate recovery by grappling (cf. Domack and Mammone, 1993). Trap array A was located near the base of the side wall of the fjord, trap array B in the bottom of the trough extending out from the ice shelf, and trap array C on a small rise on the north side of the trough about 30 m above the floor of the trough.

A sub-bottom acoustic survey was conducted from an inflatable boat using a Datasonics 3.5 kHz profiler displaying on a graphic recorder. Positions accurate to ±50 m were determined with a single global positioning system receiver and transcribed to the record manually at 1-min intervals. A total of 19.45 km of transect was run from the nearshore of Humphrey Ice Rise and the northwest coast across the fjord and within about 100 m of most of the ice face (Fig. 1).

The traps were recovered by grappling on 1 April 1999, 394 d after deployment. The first (top) trap of each array and the second trap of array B were lost or damaged sufficiently that the results could not be used reliably. The eight undamaged collectors contained columns of sediment from 150 to 280 mm high; from these the accumulation rates in millimeters per year were calculated. They were returned to the laboratory, where they were treated as short cores; after being allowed to dewater and consolidate so that they would not be damaged by handling,
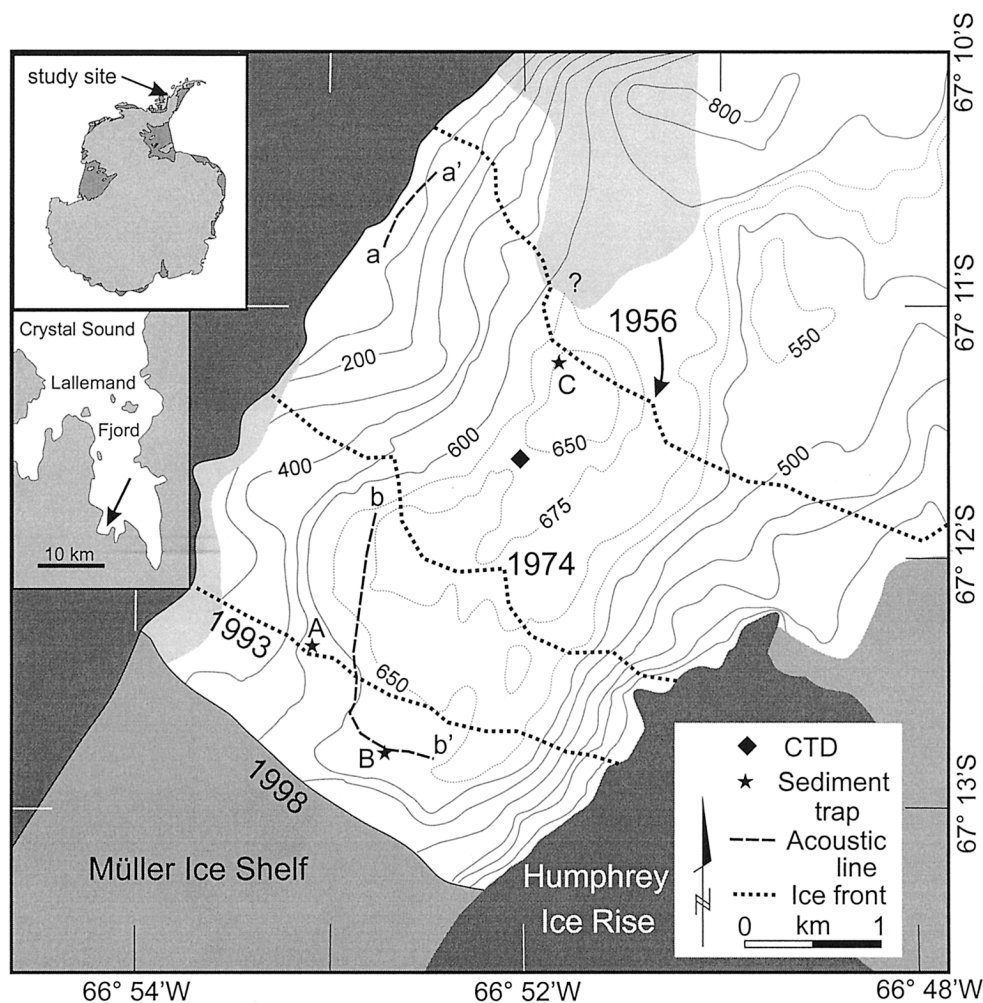
FIGURE 1. Bathymetry with locations of trap arrays and selected parts of acoustic transects (Fig. 5) in Lallemand Fjord at Müller Ice Shelf, Antarctic Peninsula. Isobaths (interval 100 m except dotted lines as marked) were drawn from a SeaBeam swath bathymetric survey in April 1999 (mainly documenting the sea floor below about 500 m depth) and an inshore 3.5 kHz sub-bottom acoustic survey from an inflatable boat in March 1998. The latter was controlled by a single GPS receiver with positions accurate to about ±50 m. Shorelines and the position of the ice front are drawn from the positions determined during the sub-bottom survey, which followed the shore within 100 m except in the western portion of the study area, where sea ice along the shore prevented access. Where isobaths are drawn in light gray areas (indicating that bathymetry is uncertain), they are estimated from Domack et al. (1995). Ice fronts before 1998 are according to Ward (1995). The ice front in 1947 was located about as in 1974.

they were split, x-rayed, logged, and subsampled. Magnetic susceptibility was determined in core and on 1.5-mL samples. Three samples from each core were dried to determine bulk density. Because there was no significant difference between values, the mean dry bulk density of 1200 kg m^{-3} was used with the volumetric accumulation rates to determine the mass accumulation rates. Particle size of deflocculated samples was determined by laser diffraction using a Malvern Master Sizer at Hamilton College. Very coarse sand (1–2 mm) and granules (>2 mm) were documented from the x-radiographs in 6-mm intervals. Biogenic silica was determined by wet alkaline extraction following Krausse et al. (1983). Organic carbon (OC) and total nitrogen (TN) content as well as OC δ^{13}C and TN δ^{15}N were analyzed using a Carlo-Erba NA-1100 analyzer coupled to a Finnigan Delta+ continuous flow mass spectrometer. Samples were dried, ground and 4 to 20 mg weighed into silver boats. Weighed samples were acidified in situ with 6% sulfurous acid to remove carbonate phases prior to isotopic analysis. Isotopic compositions were calibrated against the NBS-21 and IAEA-N1 standards that were run before and after each set of 10 analyses. Isotopic reproducibility is about 0.09‰. Sample analysis errors (1s) are generally 1% for C and N contents.

During the *N. B. Palmer* cruise in 1999, a SeaBeam swath bathymetric survey was conducted of much of the deepwater region of Lallemand Fjord. The bathymetry shown in Figure 1 is transcribed from that survey and the sub-bottom acoustic survey in 1998.

Glacimarine Setting

Müller Ice Shelf is located in an embayment on the west side of Lallemand Fjord on the Loubet coast of the Antarctic
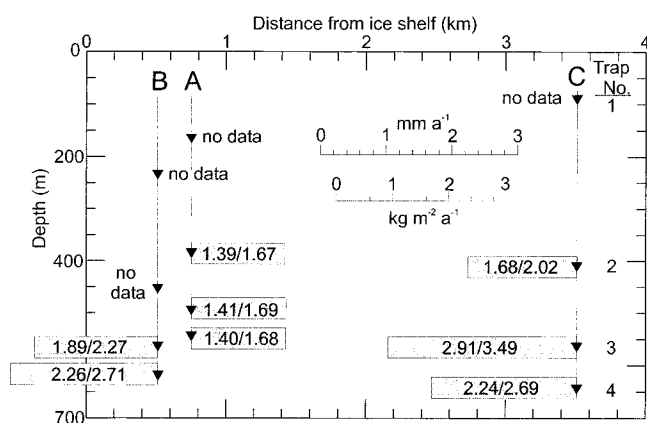
FIGURE 2. Location of the sediment traps (triangles) with respect to water depth and distance from Müller Ice Shelf front in March 1998. In each case, the sea floor was 5 m below the lowest trap. Traps are numbered from the top down as shown on the right. Bars show the accumulation of sediment in mm a^{-1} based on the volume of sediment in each trap at the time of recovery and kg m^{-2} a^{-1} based on a mean bulk density of 1200 kg m^{-3}.

R. GILBERT ET AL. / 25

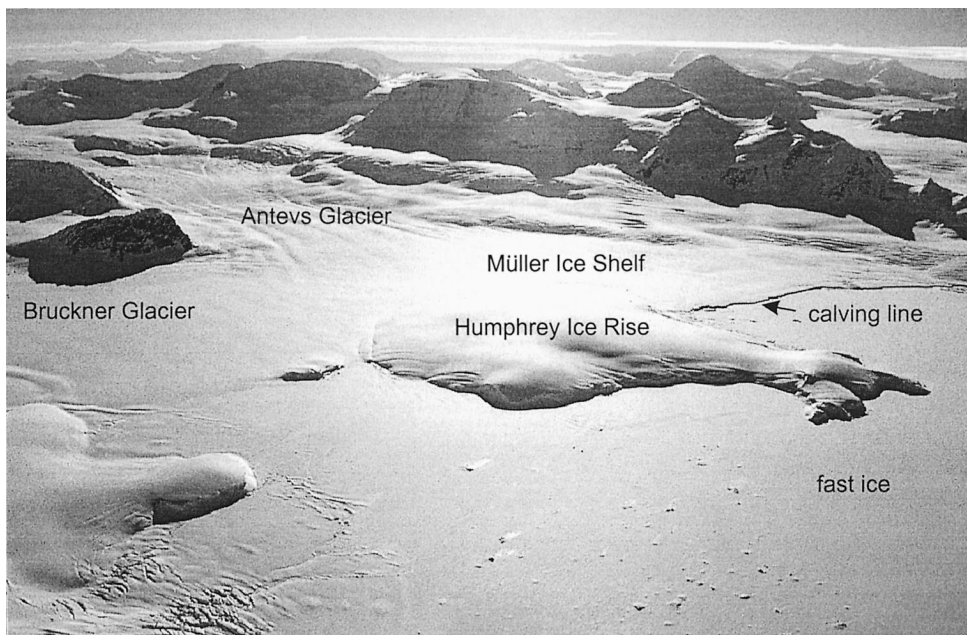*FIGURE 3. Oblique aerial view southwest over the Müller Ice Shelf to the mountains of the Arrowsmith Peninsula in November 1996 showing the Humphrey Ice Rise in the center-ground. The study site is at the right. Photograph by D. Vaughan, British Antarctic Survey.*
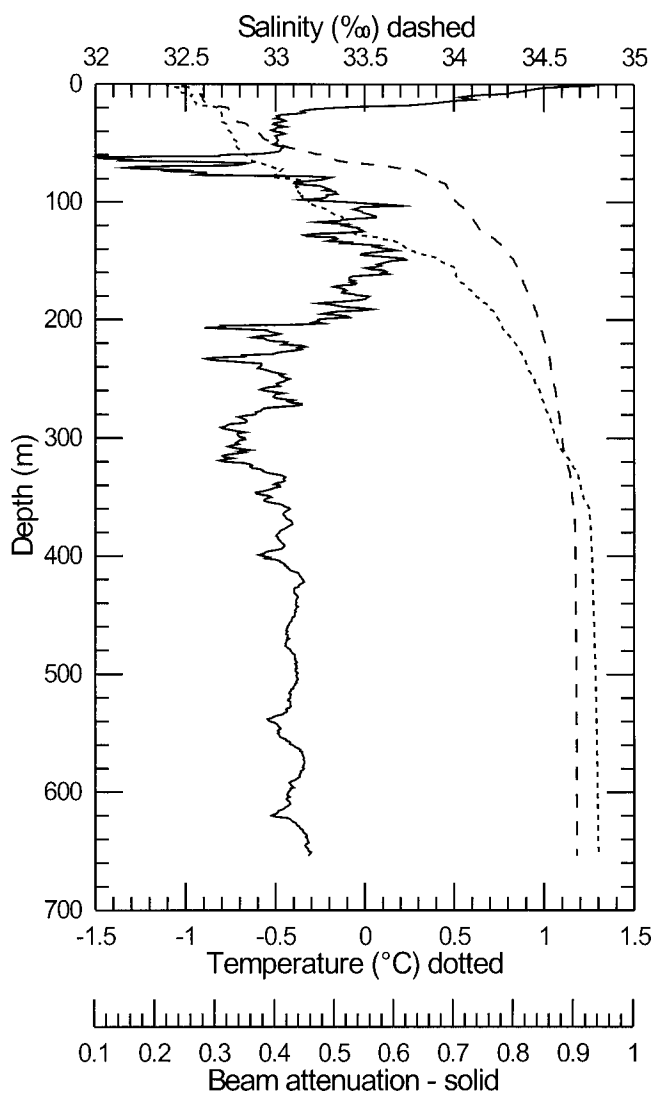

FIGURE 4. Salinity, temperature, and light attenuation cast in Lallemand Fjord at Müller Ice Shelf, 2 April 1999. For location, see Figure 1.

Peninsula at 67°13′S (Fig. 1). In 1998 it had an area of about 48 km². It is fed by Brückner and Antevs glaciers, which originate in a saddle between the Arrowsmith and Antarctic peninsulas (Fig. 3). The ice shelf divides around the Humphrey Ice Rise; it is the northwestern branch that is the focus in this study. Little is known of the glacial history of this region except that the central region of the fjord near Müller Ice Shelf was deglaciated more than 8000 yr ago (Shevenell et al., 1996).

Müller Ice Shelf may have been absent during part of the Holocene but it re-formed and advanced during the Little Ice Age (Domack et al., 1995). It is maintained by its protected setting that includes pinning on the Humphrey Ice Rise (Fig. 3). The first direct observations in 1947 placed the ice front near the 1974 position shown on Figure 1 (Ward, 1995). It advanced rapidly until about 1956, then retreated rapidly to just seaward of the 1974 position by 1963, from where it retreated slowly about 500 m until 1989 (Ward, 1995) and then more rapidly to its position when the traps were deployed in March 1998, which was 3.6 km from the location in 1956. Observations from *N. B. Palmer* in April 1999 indicated that the front had retreated 200 to 900 m from the location in 1998. Weather during this period was relatively mild; at Rothera, 100 km southwest of Müller Ice Shelf, autumn and winter mean monthly temperatures were 3 to 6 C° above the long-term average (Chong, 2000). Periodic calving of the ice shelf takes place as transverse crevasses open a few hundred meters from the terminus. We suspect these may focus eolian sediment and allow its release during calving.

The floor of Lallemand Fjord is very irregular, as a function of the bedrock beneath, glacial erosion, and a thin cover of postglacial sediment. In the mid and outer regions of the fjord isolated basins exceed 1200 m deep. Several sills occur in the fjord, including one at 550 m depth about 10 km downfjord from the Müller Ice Shelf. Apparently the sills have little effect on circulation in the fjord because warmer Circumpolar Deep Water (Hofmann et al., 1996) presently reaches Müller Ice Shelf at 100–200 m depth via Crystal Sound (Fig. 4) and contributes to its melting. Exclusion of this warm circulation may have contributed to the Little Ice Age redevelopment and advance of the shelf (Domack et al., 1995). The sea floor near Müller Ice Shelf consists of an irregular trench that deepens from a maximum of
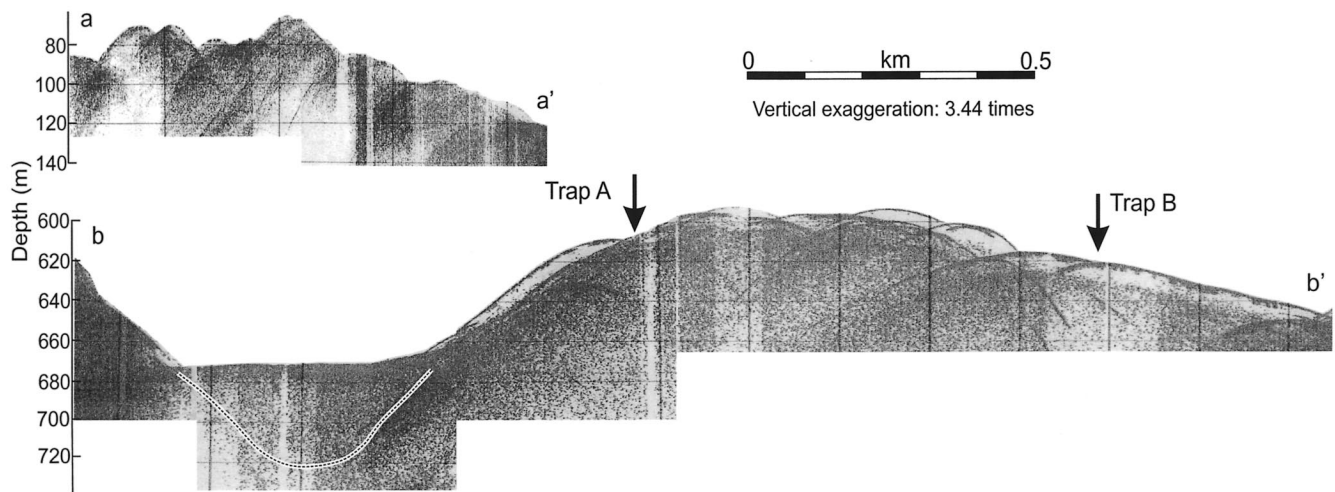
FIGURE 5. Sections of the 3.5 kHz sub-bottom acoustic record showing (a) the almost bare bedrock surface near shore and (b) the sediment cover in deep water near the front of the Müller Ice Shelf (dashed line indicates inferred bedrock reflector in depression). Depths assume sound velocity in water and sediment of 1450 m s^{-1}. Locations of the lines are shown in Figure 1. Trap array A was about 350 m west and Trap array B was about 60 m south of the nearest locations marked on b–b′.

about 570 m at the 1998 calving line through a large basin about 675 m deep to more than 800 m 6 km downfjord (Fig. 1). The height of the edge of the ice shelf above sea level (about 30 to 50 m) suggests that the relatively large section is floating where water is greater than about 500 m deep (Fig. 1).

The 3.5 kHz sub-bottom acoustic data (Fig. 5) show that the cover of sediment on the fjord floor is thin and variable. In shallow water (section a–a′) there are no sub-bottom reflectors and the surface is very irregular, indicating that bedrock is exposed with little or no sediment cover. Most of the fjord floor in deeper water (section b–b′) has a thin sediment cover of less than 10 m, indicating low rates of accumulation. This corresponds with results obtained by Shevenell et al. (1996), who documented a reservoir corrected age of 8058 ± 70 ^{14}C yr BP at 4.6 m depth (mean accumulation rate of 0.57 mm a^{-1}) in a core from about 10 km from the Ice Shelf. This sediment is acoustically transparent and contains very few internal reflectors, suggesting deposition from suspension in the water column probably both below the ice shelf and in open water before and following retreat of the ice shelf.

Depressions on the fjord floor contain thicker accumulations of sediment up to about 40 m. This material is more consolidated, or coarser grained, or both as indicated by the strength of the surface reflection and the limited depth of sound penetration. This suggests much older deposition in subglacial depressions that was preserved from scour before deglaciation of Lallemand Fjord.

Trap Records

SPATIAL PATTERNS

Data presented in this study are subject to the caveats associated with sediment trap data. In a field comparison of a number of sediment-traps designs in the deep sea, widely used conical and cylindrical traps yielded similar efficiencies (Honjo et al., 1992). Where trap collection efficiencies varied with size or shape, the most common cause is linked to turbulence associated with currents. Lallemand Fjord is a protected environment wherein we expect low current speeds and minor hydrodynamic influences on particle fluxes. In only one trap was there found a

small zooplankton "swimmer." Although there was minor bioturbation in that trap, it is unlikely that significant amounts of sediment were added or removed by its action. Dissolution of particulate matter in the receivers can result in underestimation of biogenic fluxes. However, in this setting of dominantly terrigenous sedimentation in the fjord water column and at the seabed, dissolution is unlikely to affect the flux and characteristics of the terrigenous phases that were collected.

The cone-shaped design is also consistent with that used in or near other Antarctic fjords (Dunbar et al., 1989) in order to facilitate comparison of data. Although the traps were baffled at their mouths to reduce resuspension of sediment, Gardner (1980) has shown that cones under-register accumulation by up to 20% depending on water velocity around them. As well, some sediment remains in the cone after recovery, both in the water and adhering to the sides. We measured this as averaging 2.2% of the sediment in the receivers below the traps with no pattern with respect to depth or distance from the ice shelf. It is not included in these observations, although its effect with underregistering is cumulative. However, some overestimation may have occurred because the traps collected summer sediment already suspended in the water column before they were deployed; this would counteract the under-registration. Other sources of error include interference by icebergs; clearly, traps above about 200 m depth (more than 400 m at B) were not merely jostled by passing bergs but were damaged or destroyed. In addition, sediment caught on the ropes may have fallen into the traps especially during disturbance by icebergs and when the traps were being recovered.

The total flux of sediment recorded in the traps was calculated in millimeters per year from the volume (0.23–0.43 L) measured immediately after recovery, and in kilograms per square meter per year using a mean measured bulk density of 1200 kg m^{-3} (Fig. 2). Having regard for the errors discussed above, this approximates the accumulation on the sea floor of 1 to 2 mm a^{-1} recorded by Domack and McClennan (1996), although it is significantly higher than the mean rate over 8 ka of 0.57 mm a^{-1} reported by Shevenell et al. (1996). The latter is not surprising if for much of this period Müller Ice Shelf was reduced or absent so that the clastic flux would have been lower.
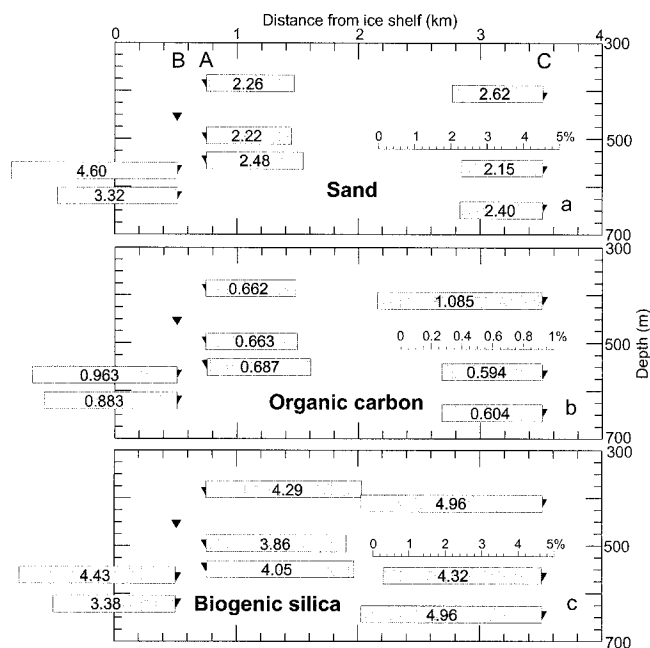
R. GILBERT ET AL. / 27

FIGURE 6. *Mean values of (a) percent sand, (b) percent organic carbon, and (c) percent biogenic silica in sediment traps. Locations with respect to depth and distance are as in Figure 2.*

Several observations arise from the accumulation data (Fig. 2). First, there is no clear trend in accumulation with distance from the ice shelf; mean rates vary from 1.40 mm a^{-1} proximally (A) to 2.28 mm a^{-1} distally (C). Accumulation is slightly lower at site A toward the side of the channel from beneath the ice shelf. Second, there is no significant difference in the accumulation with depth. If the sediment were uniformly distributed in the water column, more would be captured by lower traps because of the greater column of water above contributing by settling from suspension. The data (except for the anomalous value of 2.91 mm a^{-1} at site C) suggest that the sediment content of the water above about 400 m depth is greater than that in the bottom water. This corresponds with the CTD data (Fig. 4) which show that sediment plumes are most concentrated at the sea surface with lower concentrations in the region of increasing temperature and salinity to more than 300 m depth. Also important in this context is that the accumulation in the lowest traps (5 m above the sea floor) was the same or only slightly greater than in traps above. This may be due to resuspension from the sea floor but it does indicate that deposition from underflow (turbidity currents) was negligible during the study period.

The mean composition of sediment in the traps (Fig. 6) provides information on sedimentary processes. The texture is typical of glacimarine sediments of the fjord (Shevenell et al., 1996) with less than 5% sand, 54 to 57% silt, and 38 to 44% clay size (<4 μm). The relative amount of silt versus clay is remarkably uniform and there is no trend with distance from the ice shelf or depth in the fjord. Mean particle size varied only slightly from 11.8 μm in traps at A, to 13.1 μm at B and 12.4 μm at C, in each case increasing slightly with depth. The summer temperature of the seawater is everywhere above freezing (Fig. 4); thus, melting of the ice shelf, icebergs and sea ice occurs in the study site. A significant part of the sediment in the upper waters of the fjord, and thus in the traps, probably comes from this source, even though the glaciers feeding the shelf are cold-based and the clastic sediment component in the ice is small. It is probable that as much or more of the sediment is

contributed from eolian processes. Weathering of relatively small areas of exposed bedrock in the region (Fig. 3) provides a source for limited eolian transport, and the 30–50-m-high ice cliff at the edge of the shelf shelters the sea surface nearby, especially from downvalley katabatic winds, facilitating deposition. The relatively uniform distribution of sand with depth also suggests a source at the surface, or in the upper reaches of the water column, rather than by transport along the sea floor. No measurements have been made of eolian sediment on the sea ice, although a slight darkening was observed on the snow on parts of the ice shelf. Elsewhere around Antarctica, there are extensive eolian deposits in similar environments (Barrett et al., 1983).

Most of the sediment is clastic, with less than 1% organic carbon, and about 5% biogenic silica (Figs. 6b, c). There is little to distinguish these variables with respect to depth or distance, suggesting that the source of autochthonous organic material is in the upper part of the water column, and that organic processes do not differ greatly throughout the study area. The organic carbon values are comparable to those in sediments of the Ross Sea (Dunbar et al., 1985), the continental shelf of the Antarctic Peninsula (Leventer et al., 1996), and the outer reaches of fjords elsewhere on the Antarctic Peninsula (Domack et al., 1993; Domack and Ishman, 1993). However, they are only 15 to 32% of values in sediments from similar traps in Andvord Bay (Domack and Mammone, 1993) but they are up to 5 times the values in sediments near the trap locations in Lallemand Fjord and up to 2 times the amounts found in sediments from near the mouth of the fjord (Domack et al., 1995; Domack and McClennan, 1996). This downfjord increase in organic matter content represents dilution in the ice shelf proximal region by clastic material (Domack et al., 1994). Biogenic silica values are 13 to 27% of the values from traps in Andvord Bay (Domack and Mammone, 1993). They are comparable to those in the sediments of the eastern Ross Sea but are very much lower than those in the western Ross Sea and McMurdo Sound (Dunbar et al., 1985), where winnowing from shallow water focuses biogenic detritus (Dunbar et al., 1989), and in Andvord Bay, Antarctic Peninsula (Domack et al., 1993).

The product of the biogenic content (Fig. 6) and the mass accumulation rates (Fig. 2) provides an estimate of the biogenic flux. Values for organic carbon were highest at sites B (22–24 g m^{-2} a^{-1}) and C (16–22 g m^{-2} a^{-1}) and lowest at site A (11 g m^{-2} a^{-1}). Biogenic silica fluxes followed a similar pattern: 92–100 g m^{-2} a^{-1} at B, 100–151 g m^{-2} a^{-1} at C and 68–72 g m^{-2} a^{-1} at A. These values may be compared with daily fluxes from trap studies in the open waters of Bransfield Strait to the northwest of the Antarctic Peninsula of 0.98 mg m^{-2} d^{-1} at 500 m depth and 51 mg m^{-2} d^{-1} at 1000 m depth (Anadón and Estrada, 2002; Palanques et al., 2002).

TEMPORAL VARIATIONS

Figures 7, 8, and 9 show the temporal patterns of measured variables. In the discussion below it is assumed that the bottom of each sediment column contains sediment deposited shortly after deployment toward the end of the austral summer, that sediment in midcore represents winter deposition, and that sediment near the top was deposited during the following spring and summer. However, the rates of accumulation were almost certainly not constant through this period, and because intervalometers were not available in this study, precise dates cannot be assigned through the sediment columns. In Figures 8 and 9 the physical properties are plotted with respect to relative depth (as a percentage of the total depth) in each sediment column. This allows

comparison between sites assuming that the rate of accumulation with respect to time varied by roughly the same amount in all traps. It also removes the effect of shrinkage (4 to 28%) which occurred as a result of allowing the sediment columns to dewater and consolidate, assuming the rate was about the same everywhere in the core.

The x-radiographs (Fig. 7) show that sediment is faintly laminated to massive through the period of record. Where faint laminations are present in several traps, most notably A4 (Fig. 7), B3 and C4, they occur as very thin (0.2–0.5 mm) wispy partings of darker tone (less x-ray transmission, indicating coarser particle size, or greater clastic content, or lower water content). The normalized gray-scale of the x-radiograph revealed 21 prominent dark peaks and 30 lesser but clearly recognizable peaks in the record (mean thickness 1.5 mm, standard deviation 0.73 mm). Laminae are more prominent in the upper part of the cores, which may represent events in spring and into summer. Wave data from the U.S. Fleet Numerical Meteorology and Oceanography Center (FNMOC, 2001) indicate that about 60 to 80 storms cross the Antarctic Peninsula per year, generating wave heights in ice-free waters of 11 m or more. It is possible that storm surges into Lallemand Fjord, even under sea ice, subtly influence the distribution or input of sediment in the water column sufficiently to create the laminae. In addition, the 27 cycles of spring and neap tides during the period of deployment may be recorded in these laminae as a response to more vigorous circulation during the spring tidal cycle. It is unlikely that these laminae would be recognized in cores, given their mean thickness would be about 0.015 mm, that is, not much greater than the mean particle diameter.

The sediment is marginally coarser toward the tops and bottoms of the cores (Fig. 8b). The sand content (Fig. 8c), representing eolian input and ice-rafted debris is markedly greater in summer, although ice rafting of very coarse sand and granules (Figs. 8d and e) occurs through the year. The peak in very coarse sand in midsection (interpreted as winter) may also represent eolian loading through fractured sea ice during winter, during the time of reduced input of fine sediments. McKenna Neuman (1993) has shown that in arctic fjord environments, much of the eolian transport occurs in winter during intense storms associated with sublimation of ice-cemented deposits, and is facilitated by blowing snow. The particle size distributions (Fig. 9) of the finer sediment fraction (<0.6 mm) show similar patterns throughout, with somewhat more leptokurtic sediments in the upper parts of the traps. The small secondary peaks in midsand size, especially toward the tops and bottoms, reflect the eolian and IRD components. Otherwise, there is little to distinguish the texture of the fine sediments deposited through the year.

The organic matter content of the traps shows a pronounced seasonal distribution. The fraction of nitrogen (Fig. 8f) is less than about 0.1% in winter sediments but with several exceptions increases to about 0.2 to 0.3% in summer, with the greatest accumulation at the end of summer and probably into the beginning of winter. With one exception in trap B3, organic carbon (Fig. 8h) is about 0.3 to 0.6% in winter and as high as 2.5% in summer. The lower levels in the midsections of the traps presumably represent winter through summer heterotrophic consumption of the previous season's delivery of organic matter to the water column and the sea floor. This consumption preferentially removes ^{12}C relative to ^{13}C and ^{14}N relative to ^{15}N. C/N ratios (not shown) are in the range 5 to 10 with no seasonal differences, which is close to the Redfield ratio for fresh Antarctic plankton. Carbon content is higher than reported by Domack et al. (1995) and Shevenell et al. (1996) from cores nearby
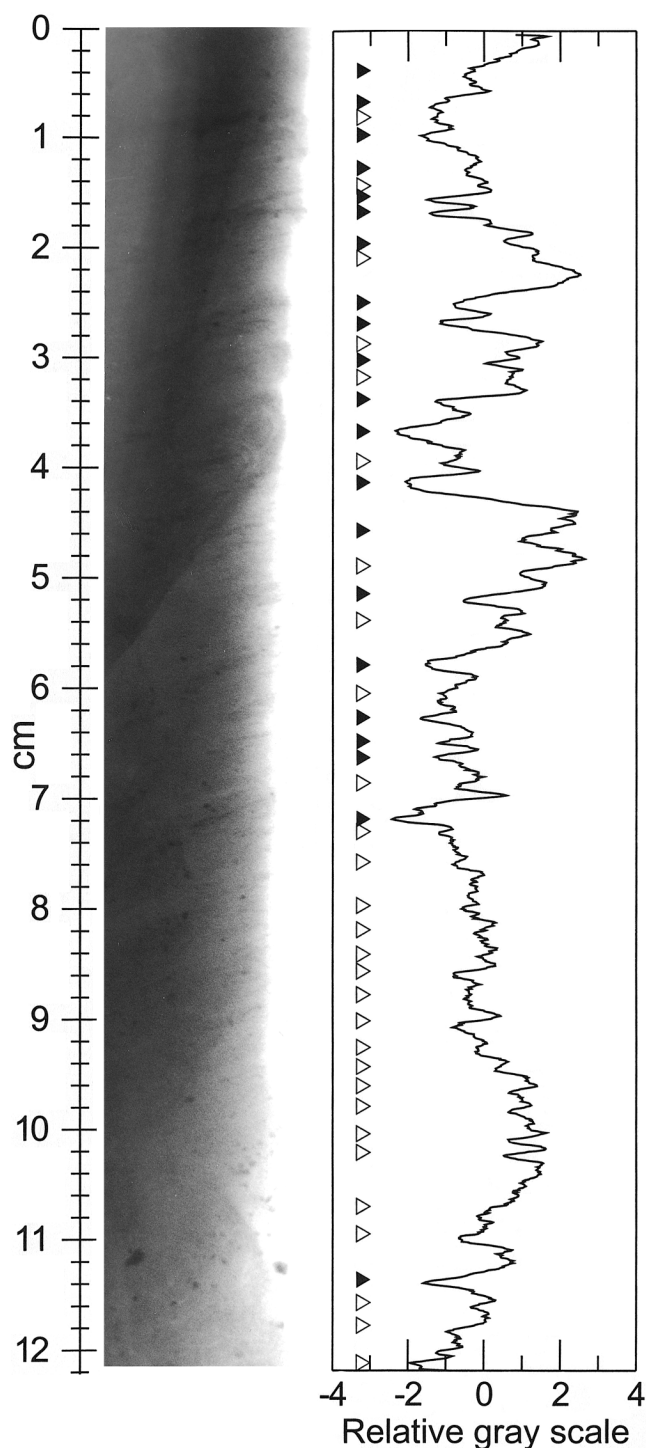

FIGURE 7. *Positive x-radiograph (dark represents less penetration of x-rays) of sediment in Trap A4. Tonal changes are indicated by a normalized gray scale calculated from gray-scale values averaged over 0.5 cm width of the core, detrended linearly, and expressed as standard deviations from the mean. The effect of solitary large particles as dark objects was removed from the gray-scale plot. Prominent (solid triangles) and lesser (open triangles) darker laminae were assigned arbitrarily based on examination of the image and the peaks in gray scale.*

in Lallemand Fjord, likely because of carbon recycling by benthos on the sea floor, or increased biogenic carbon production in an ameliorating climate.

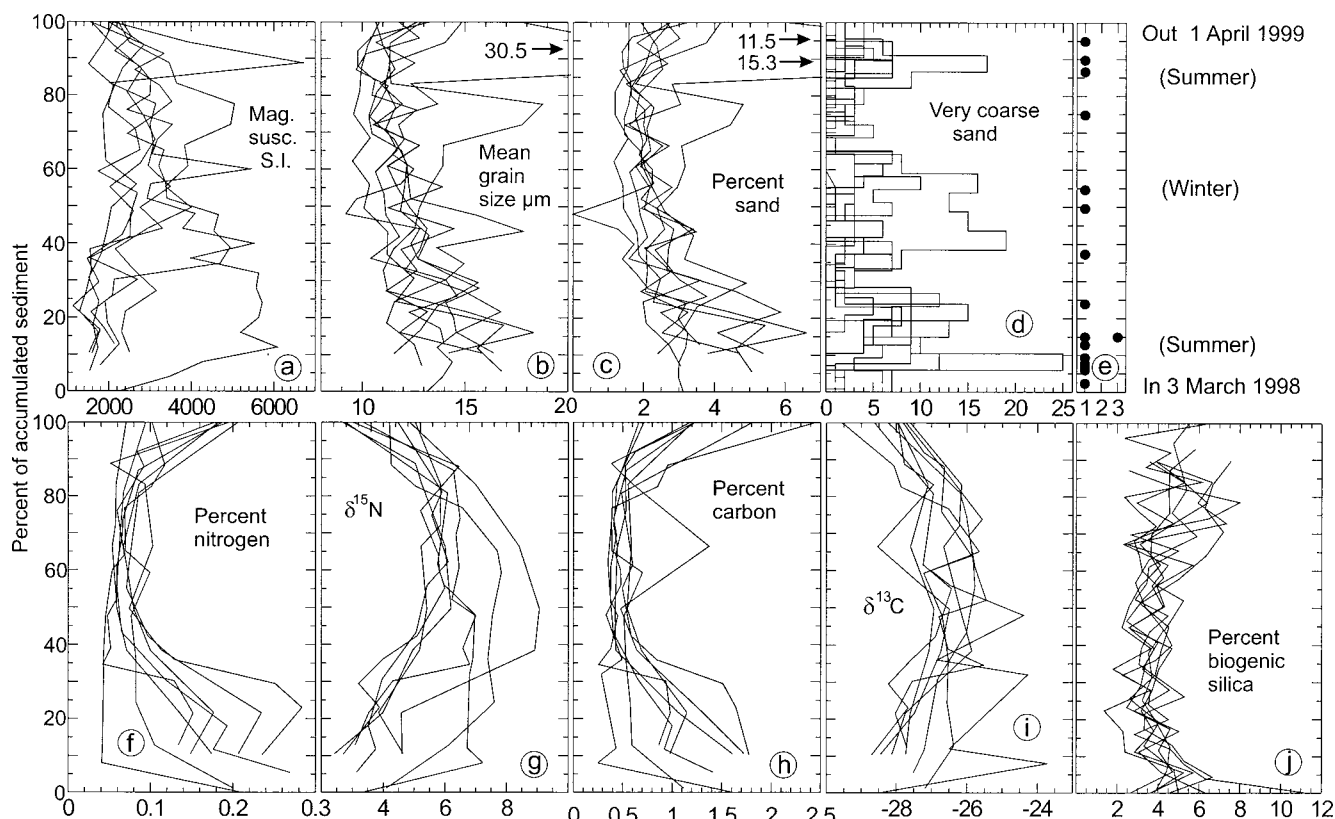Biogenic silica (Fig. 8j) is about the same throughout the

R. GILBERT ET AL. / 29

FIGURE 8. Measured parameters from the sediment trap samples: (a) magnetic susceptibility in S.I. units, (b) Mean particle size in μm, (c) percent sand (>62.5 μm), (d) number of very coarse sand particles (1–2 mm) in 6-mm increments, (e) number of particles larger than 2 mm diameter in 6-mm increments, (f) percent nitrogen, (g) $\delta^{15}N$, (h) percent organic carbon, (i) $\delta^{13}C$, and (j) percent biogenic silica. In each case the accumulations are presented as relative amounts of accumulation to facilitate comparison between traps.

deposit, with only slightly higher values centered at about 80% accumulated sediment. This may be associated with the diatom bloom in the early part of the summer. Lallemand Fjord is ice covered during much of the year and it is probable that sea ice diatoms contribute to the Si flux. Using sediments and trap samples from McMurdo Sound, Leventer and Dunbar (1987) found that most sea ice diatom species, once released from the ice habitat, dissolve in the water column at the seabed. Only heavily silicified forms such as *Fragilariopsis curta,* which also occur in open water or bloom at the ice edge, are found preserved in sediments beneath areas of summer sea ice cover. The results from Lallemand Fjord are consistent with significant diatom production but minimal seabed preservation, indicative of a low flux of heavily silicified diatom species. The significant fraction of biogenic silica, up to 11%, is much greater than the trace amounts accumulated during the past 2100 yr found in cores from the area, again reflecting recycling or greater recent production. However, this is equivalent to elevated levels preceding about 2500 BP (Shevenell et al., 1996; Taylor et al., 2001), suggesting greater marine productivity at that time.

Total particulate $\delta^{15}N$ (Fig. 8g) likewise changes in response to heterotrophic removal of the lighter isotope [14]N. Freshly produced and delivered organic matter has lower $\delta^{15}N$. It is also possible that the higher $\delta^{15}N$ values also represent increased contribution from higher tropic levels (zooplankton are 3 to 4‰ enriched relative to algae) during the winter months.

Particulate organic $\delta^{13}C$ in Southern Ocean coastal waters is a useful tracer of organic matter provenance, with sea ice providing organic matter in the range of −22 to −8‰, versus open water systems producing organic matter ranging from −23 to −32‰ (Rau et al., 1991; Dunbar and Leventer, 1993; Gibson et al., 1999; Villinski et al., 2000). Furthermore, in the Ross Sea ice-edge diatom blooms tend to produce organic matter in the range of −23 to −27‰, whereas algal communities in deeply mixed open water environments tend to be somewhat more negative (Villinski et al., 2000). Organic matter $\delta^{13}C$ from the Lallemand Fjord sediment traps ranges from −23 to nearly −30‰, with most samples falling within 1‰ of −27‰. Based on the Ross Sea work, these values are consistent with relatively low productivity in the ice-edge environment, most likely dominated by diatoms.

Weight percent C and N are higher and OC $\delta^{13}C$ and TN $\delta^{15}N$ are lower in the lowermost 30% and the uppermost 10% of accumulated sediment in the traps (Fig. 8g and i), consistent with enhanced organic matter flux during the summer to autumn bloom and flux period of 1998 and 1999. Because C/N ratios are mostly close to the Redfield values for fresh antarctic plankton throughout the collection period, it is unlikely that old, autochthonous or reworked organic matter contributes to the sediment flux that we observed. Nevertheless, the stable isotopic data suggest that some remineralization or food chain recycling of organic matter is occurring. The increase of OC $\delta^{13}C$ and TN $\delta^{15}N$ during the winter period (from 40 to 85% of the accumulated sediment in Fig. 8) is consistent with the loss of the lighter isotope through bacterial remineralization or enrichment in the heavier isotope via uptake into zooplankton.
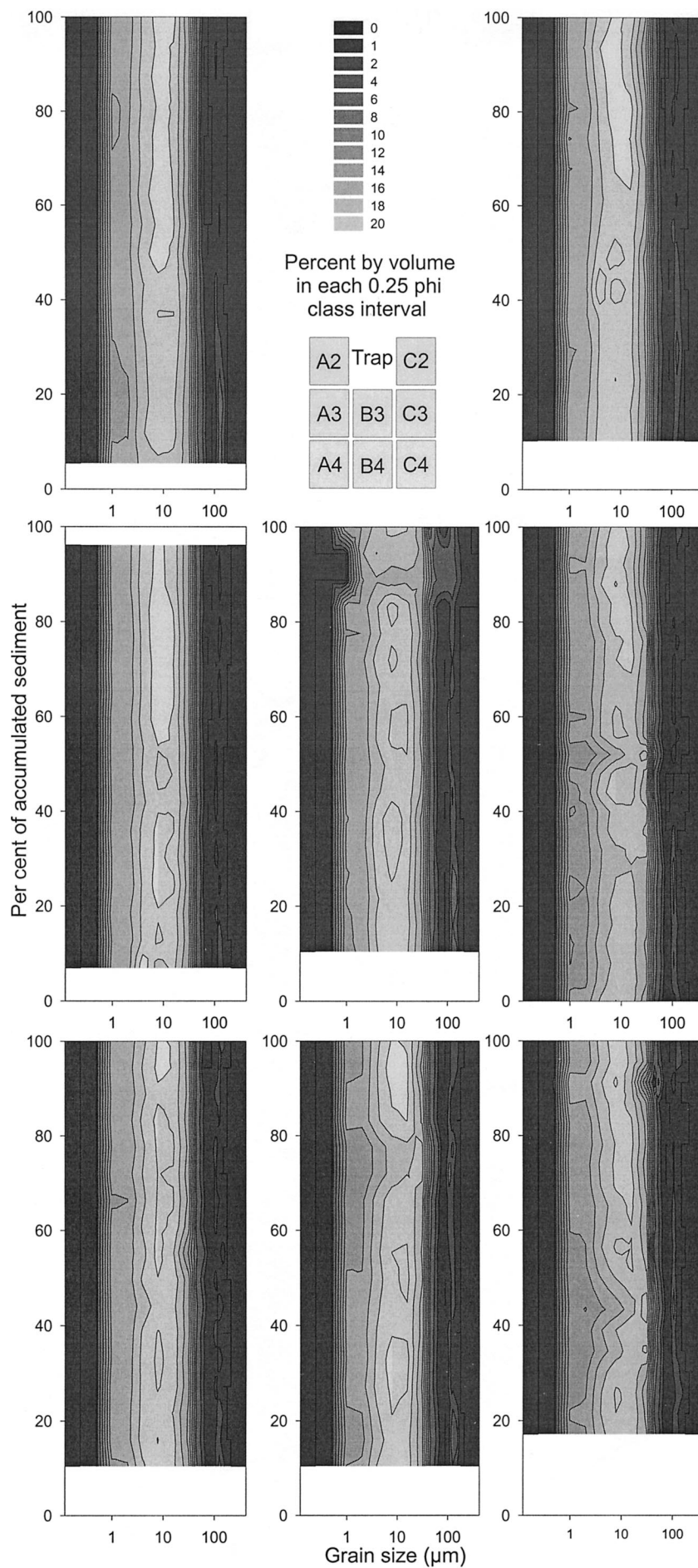
FIGURE 9. Particle size distributions (Beierle et al., 2002) for particles less than 600 μm in each sediment trap.

R. GILBERT ET AL. / 31

Conclusions

Sediment trap records provide an indication of the spatial and temporal flux of clastic and organic matter near the face of an antarctic ice shelf. The most important findings are the following.

The flux of sediment is relatively uniform with respect to distance from the ice shelf, lateral position in the fjord, and depth of water and relief of the sea floor. This indicates the predominance of an equally distributed sediment source in the upper part of the water column as is confirmed by the CTD data. Benthic processes, including turbidity current flow and biogenic or colluvial resuspension, play a relatively minor role in the sedimentary environment. The principal sources of clastic sediment are associated with melt of debris-poor ice of the shelf and the bergs it produces, and with eolian transport from limited exposed bedrock in the vicinity. The latter is facilitated by the sheltering and trapping effect in the lee of the front of the ice shelf.

The fluxes recorded in 1 yr from the traps are within a factor of 2 or 3 of what has been determined by dating cores of nearby seafloor sediments over most of the Holocene. This approximation is remarkable considering the potential for physical and biochemical diagenetic changes in the seafloor sediments, and for changes in sediment flux associated with changing environmental conditions, including climatic and glacial processes, especially related to the location of the front of the ice shelf.

There is a strong seasonal component in most of the physical parameters measured in the cores. Although we are not able to date events within the cores (except the tops and bottoms), the distinction between winter and summer conditions is apparent. Sand content is higher in summer due to increased melting and release of glacial and eolian sediment. However, a secondary peak in very coarse sand during winter is inferred to relate to input of eolian sediment throughout the year and release through leads in sea ice, especially during stormy conditions.

The same seasonality is apparent in the biological components. Carbon and nitrogen values are higher in the upper and lower parts of the trap records, representing increased summer flux. The isotopic OC $\delta^{13}C$ and TN $\delta^{15}N$ values are lower during these periods associated with loss of lighter isotopes through bacterial remineralization or enrichment in heavier isotopes due to uptake by zooplankton.

Acknowledgments

References Cited

Anadón, R., and Estrada, M., 2002: The FRUELA cruises: A carbon flux study in productive areas of the Antarctic Peninsula (December 1995–February 1996). *Deep Sea Research II,* 49: 567–583.

Barrett, P. J., Pyne, A. R., and Ward, B. L., 1983: Modern sedimentation in McMurdo Sound, Antarctica. *In*: Oliver, R. L., James, P. R., and Jago, J. B. (eds.), *Antarctic Geoscience.* Canberra: Australian Academy of Science, 550–554.

Beierle, B. D., Lamoureux, S. F., Cockburn, J. M. H., and Spoo-ner, I., 2002: A new method for visualizing sediment particle size distributions. *Journal of Paleolimnology,* 27: 279–283.

Chong, Å., 2000: Sediment trap records of deposition in Lallemand Fjord adjacent to Müller Ice Shelf, Antarctic Peninsula. M.Sc. thesis, Queen's University, Kingston. 105 pp.

Domack, E. W., Foss, D. J. P., Syvitski, J. P. M., and McClennen, C. E., 1994: Transport of suspended particulate matter in an Antarctic fjord. *Marine Geology,* 121: 161–170.

Domack, E. W., and Ishman, S., 1993: Oceanographic and physiographic controls on modern sedimentation within Antarctic fjords. *Geological Society of America, Bulletin,* 105: 175–1189.

Domack, E. W., Ishman, S. E., Stein, A. B., McClennan, C. E., and Jull, A. J. T., 1995: Late Holocene advance of the Müller Ice Shelf, Antarctic Peninsula: sedimentological, geochemical and palaeontological evidence. *Antarctic Science,* 7: 159–170.

Domack, E., Leventer, A., Gilbert, R., Brachfeld, S., Ishman, S., Camerlenghi, A., Graham, K., Carlson, D., and Barkoukis, A., 2001: Cruise reveals history of Holocene Larsen Ice Shelf. *Eos, Transactions of the American Geophysical Union,* 82: 13 and 16–17.

Domack, E. W., and Mammone, K. A., 1993: Modern sedimentation within Andvord Bay, Antarctic Peninsula. *Antarctic Journal of the United States,* 28: 97–98.

Domack, E. W., Mashiotta, T. A., and Burkley, L. A., 1993: 300-year cyclicity in organic matter preservation in Antarctic fjord sediments. *The Antarctic Paleoenvironment: A Perspective on Global Change,* 60: 265–272.

Domack, E. W., and McClennen, C. E., 1996: Accumulation of glacial marine sediments in fjords of the Antarctic Peninsula and their use as late Holocene Paleoenvironmental indicators. *Foundations for Ecological Research West of the Antarctic Peninsula.* Antarctic Research Series, 70: 135–154.

Dunbar, R. B., Anderson, J. B., and Domack, E. W., 1985: Oceanographic influences on sedimentation along the antarctic continental shelf. *Oceanology of the Antarctic Continental Shelf,* Antarctic Research Series, 43: 291–312.

Dunbar, R. B., and Leventer, A. R., 1993: Seasonal variation in carbon isotopic composition of Antarctic sea ice and open water plankton communities. *Antarctic Journal of the United States,* 27: 79–81.

Dunbar, R. B., Leventer, A. R., and Stockton, W. L., 1989: Biogenic sedimentation in McMurdo Sound, Antarctica. *Marine Geology,* 85: 155–179.

FNMOC (Fleet Numerical Meteorology and Oceanography Center), 2001: www.fnmoc.navy.mil

Gardner, W. D., 1980: Sediment trap dynamics and calibration: a laboratory evaluation. *Journal of Marine Research,* 38:17–39.

Gibson, J. A. E., Trull, T., Nichols, P. D., Summons, R. E., and McMinn, A., 1999: Sedimentation of ^{13}C-rich organic matter from Antarctic sea ice algae: a potential indicator of past sea-ice presence. *Geology,* 27: 331–334.

Hofmann, E. E., Klinch, J. M., Lascara, C. M., and Smith, D. A., 1996: Water mass distribution and circulation west of the Antarctic Peninsula and including Bransfield Strait. *Foundations for Ecological Research West of the Antarctic Peninsula.* Antarctic Research Series, 70: 61–80.

Honjo, S., Spenser, D. W., and Gardner, W. D., 1992. A sediment trap intercomparison experiment in the Panama Basin, 1979. *Deep-Sea Research,* 39: 333–358.

Krausse, G. L., Schelske, C. L., and Davis, C. O., 1983: Comparison of the wet-alkaline methods of digestion of biogenic silica in water. *Freshwater Biology,* 13: 73–81.

Leventer, A., Domack, E. W., Ishman, S. E., Brachfeld, S., McClennen, C. E., and Manley, P., 1996: Productivity cycles of 200–300 years in the Antarctic Peninsula region: understanding linkages among the sun, atmosphere, oceans, sea ice, and biota. *Geological Society of America, Bulletin,* 108: 1626–1644.

Leventer, A., and Dunbar, R. B., 1987: Diatom flux in McMurdo Sound, Antarctica. *Marine Micropaleontology,* 12: 49–64.

McKenna Neuman, C., 1993: A review of aeolian transport processes in cold environments. *Progress in Physical Geography,* 17: 137–155.

Palanques, A., Isla, E., Puig, P., Sanchez-Cabeza, J. A., Masqué, P., 2002: Annual evolution of downward particle fluxes in the Western Bransfield Strait (Antarctica) during the FRUELA project. *Deep-Sea Research II,* 49: 903–920.

Rau, G. H., Sullivan, C. W., and Gordon, L. I., 1991: Variations in Weddell Sea particulate organic matter. *Marine Chemistry,* 35: 355–369.

Scambos, T. A., Hulbe, C., Fahnstrock, M., and Bohlander, J., 2001: The link between climate warming and break-up of ice shelves in the Antarctic Peninsula. *Journal of Glaciology,* 154: 516–530.

Shevenell, A. E., Domack, E. W., and Kernan, G. M., 1996: Record of Holocene palaeoclimate change along the Antarctic Peninsula: evidence from glacial marine sediments, Lallemand Fjord. *Papers and Proceedings of the Royal Society of Tasmania,* 130: 55–64.

Skvarca, P., Rack, W., Rott, H., and Donangelo, T. I. Y., 1999: Climatic trend and the retreat and disintegration of ice shelves on the Antarctic Peninsula: an overview. *Polar Research,* 18: 151–157.

Taylor, F., Whitehead, J., and Domack, E., 2001: Holocene paleoclimate change in the Antarctic Peninsula: evidence from the diatom, sedimentary and geochemical record. *Marine Micropaleontology,* 41: 25–43.

Villinski, J. C., Dunbar, R. B., and Mucciarone, D. A., 2000: $^{13}C/^{12}C$ ratios of sedimentary organic matter from the Ross Sea, Antarctic: a record of sea ice and open water phytoplankton bloom dynamics. *Journal of Geophysical Research,* 105: 14,163–14,172.

Ward, C., 1995: Mapping ice front changes of Müller Ice Shelf, Antarctic Peninsula. *Antarctic Science,* 7: 197–198.